Influence of dipolar defects on switching behavior in ferroelectrics

Rajeev Ahluwalia and Wenwu Cao
Materials Research Laboratory, The Pennsylvania State University, University Park, Pennsylvania 16802
(Received 25 July 2000; published 11 December 2000)

By including the contributions of dipolar defects in the time-dependent Ginzburg-Landau theory, we have simulated the domain switching process in ferroelectrics. The model incorporates elastic effects in the form of an anisotropic long-range interaction that is obtained by integrating out the strain fields, subject to the elastic compatibility constraint. The defects are simulated by considering an inhomogeneous electric field due to randomly placed coarse-grained dipoles. It is shown that these defects act as nuclei for the formation of 90° twinned structures, resulting in a lower coercive field compared to the defect-free case. Due to these defects, the simulated polarization switching occurs by two successive 90° rotations, rather than a single 180° flipping as in the defect-free case.

DOI: 10.1103/PhysRevB.63.012103 PACS number(s): 77.80.Dj, 64.70.Kb, 77.80.Fm

The spontaneous polarization in ferroelectrics can be reversed when a strong electric field is applied opposite to the polarization direction. It is crucial to understand the details of this switching process in order to produce better materials for memory devices. It has been recognized that the switching process is influenced by the presence of defects which are present in the form of vacancies and dopants.[1] Due to the localized nucleation of domains of reversed polarization, the experimentally measured coercive field is usually smaller than the *intrinsic* value predicted by the simple one-dimensional (1D) Landau theory. A recent work indicated that the *intrinsic* coercive field can be realized in a Langmuir-Blodgett polymer film, which is thin enough to bypass localized nucleation.[2]

The exact mechanism of polarization switching is, however, still lacking at the moment. Although some interesting simulations on defect-free systems have been reported,[3] a more realistic model is needed, which can take into account the defect nucleation and the motion of domain walls, as well as the influence of elastic strain.

Time-dependent Ginzburg-Landau (TDGL) equations have been used to study pattern formation in ferroelectrics.[4–6] These works, however, have focused only on the domain pattern formation aspects and did not attempt to describe switching phenomena and the role played by defects. In this paper, we report a simulation study of polarization switching in ferroelectrics, based on the TDGL approach. Specifically, we will address the issue of nucleation from localized dipolar defects and the influence of elastic long-range interactions.

The 3D Ginzburg-Landau free energy for ferroelectric systems has been given before.[7] In this work, we restrict ourselves to a 2D system undergoing a square to rectangle transition, which is analogous to the cubic to tetragonal phase transition in 3D. The total free energy is written as

$$F=\int d\vec{r}[f_l+f_g+f_{el}+f_{es}+f_{ext}+f_d], \tag{1}$$

where f_l is the local free-energy density given by

$$f_l=\frac{\alpha_1}{2}(P_x^2+P_y^2)+\frac{\alpha_{11}}{4}(P_x^4+P_y^4)+\frac{\alpha_{12}}{2}P_x^2P_y^2, \tag{2}$$

and f_g is the gradient energy,

$$f_g=\frac{g_1}{2}\left[\left(\frac{\partial P_x}{\partial x}\right)^2+\left(\frac{\partial P_y}{\partial y}\right)^2\right]+\frac{g_2}{2}\left[\left(\frac{\partial P_x}{\partial y}\right)^2+\left(\frac{\partial P_y}{\partial x}\right)^2\right]+g_3\left(\frac{\partial P_x}{\partial x}\right)\left(\frac{\partial P_y}{\partial y}\right). \tag{3}$$

It has been shown that the gradient energy may be obtained as a local approximation to the dipole-dipole interactions.[1] The term f_{el} represents the usual elastic energy of the square system. We consider the bulk strain $\phi_1=(\eta_{xx}+\eta_{yy})/\sqrt{2}$, deviatoric strain $\phi_2=(\eta_{xx}-\eta_{yy})/\sqrt{2}$, and shear strain $\phi_3=\eta_{xy}=\eta_{yx}$. Here η_{ij} is the linear elastic strain tensor given as $\eta_{ij}=\frac{1}{2}(\partial u_i/\partial x_j+\partial u_j/\partial x_i)$. The elastic free energy can then be written as

$$f_{el}=\frac{a_1}{2}\phi_1^2+\frac{a_2}{2}\phi_2^2+\frac{a_3}{2}\phi_3^2, \tag{4}$$

where a_1, a_2, and a_3 are constants that can be expressed in terms of linear combinations of elastic constants of the system. The coupling energy f_{es} may be written as

$$f_{es}=-q_1\phi_1(P_x^2+P_y^2)-q_2\phi_2(P_x^2-P_y^2)-q_3\phi_3P_xP_y. \tag{5}$$

Here q_1, q_2, and q_3 are constants that are related to the electrostrictive constants of the system. The term f_{ext} is given by $f_{ext}=-\vec{E}_{ext}\cdot\vec{P}$. The amplitude of field $\vec{E}_{ext}$ is a tunable parameter in our simulations for studying polarization switching. The term f_d represents the free-energy contribution due to randomly distributed coarse-grained dipolar defects given as $f_d=-\vec{E}_d\cdot\vec{P}$, where $\vec{E}_d=-\vec{\nabla}V_d$. The potential V_d represents a configuration of randomly placed dipoles given as

$$V_d(\vec{r}_i)=\sum_j^{n_d}\left[\frac{q_0(\vec{r}_j)}{|\vec{r}_i-(\vec{r}_j+\vec{\delta}_j)|}-\frac{q_0(\vec{r}_j)}{|\vec{r}_i-(\vec{r}_j-\vec{\delta}_j)|}\right]. \tag{6}$$

Here $q_0(\vec{r}_j)$ represents the coarse-grained charge and $\vec{\delta}(\vec{r}_j)$ the displacement associated with the defect dipole centered

at $\vec{r}_j$. We assume that the system reaches mechanical equilibrium very fast so that we may integrate out the elastic fields, subject to the elastic compatibility constraint.[8] In terms of the strain components ϕ_1, ϕ_2, and ϕ_3, the elastic compatibility relation is given as

$$\nabla^2\phi_1-\left(\frac{\partial^2}{\partial x^2}-\frac{\partial^2}{\partial y^2}\right)\phi_2-\sqrt{8}\,\frac{\partial^2}{\partial x\partial y}\,\phi_3=0. \tag{7}$$

To incorporate the elastic compatibility constraint, we consider an effective elastic part of the free energy $F_{eff}=F_{el}+F_{es}+F_{cons}$, with Lagrangian multiplier λ, where

$$F_{el}=\int d\vec{k}\left\{\frac{a_1}{2}|\phi_1(\vec{k})|^2+\frac{a_2}{2}|\phi_2(\vec{k})|^2+\frac{a_3}{2}|\phi_3(\vec{k})|^2\right\}, \tag{8}$$

$$F_{es}=-\int d\vec{k}\{q_1\Gamma_1(\vec{k})\phi_1(-\vec{k})+q_2\Gamma_2(\vec{k})\phi_2(-\vec{k})+q_3\Gamma_3(\vec{k})\phi_3(-\vec{k})\} \tag{9}$$

$$F_{cons}=\int d\vec{k}\{\lambda(\vec{k})[-k^2\phi_1(-\vec{k})+(k_x^2-k_y^2)\phi_2(-\vec{k})+\sqrt{8}k_xk_y\phi_3(-\vec{k})]\}. \tag{10}$$

Here $k^2=k_x^2+k_y^2$ and $\Gamma_1(\vec{k})$, $\Gamma_2(\vec{k})$, and $\Gamma_3(\vec{k})$ are, respectively, the Fourier transforms of $P_x^2+P_y^2$, $P_x^2-P_y^2$, and P_xP_y. The condition of mechanical equilibrium and the compatibility relation demands $\delta F_{eff}/\delta\phi_i=0$ $(i=1,2,3)$ and $\delta F_{eff}/\delta\lambda=0$. Since the square to rectangular transition does not involve shear strain and the bulk strain is isotropic, the first and third terms in Eq. (5) do not have much influence on the characteristics of the domain formation. For computational simplicity, we will consider only the deviatoric strain coupling, i.e., $q_1\to 0$ and $q_3\to 0$; using the equilibrium conditions, the free energy F_{eff} can be expressed in Fourier space as

$$F_{eff}=\frac{q_2^2}{2a_2}\int d\vec{k}H(\vec{k})|\Gamma_2(\vec{k})|^2, \tag{11}$$

where $H(\vec{k})=[h_1^2(\vec{k})/\alpha+h_2^2(\vec{k})-2h_2(\vec{k})+h_3^2(\vec{k})/\beta]$. The quantities $h_1(\vec{k})=k^2Q(\vec{k})$, $h_2(\vec{k})=\{1-(k_x^2-k_y^2)Q(\vec{k})\}$, and $h_3(\vec{k})=-\sqrt{8}k_xk_yQ(\vec{k})$, with $Q(\vec{k})$ defined as

$$Q(\vec{k})=\frac{(k_x^2-k_y^2)}{[k^4/\alpha+(k_x^2-k_y^2)^2+8k_x^2k_y^2/\beta]}. \tag{12}$$

We have introduced the dimensionless constants $\alpha=a_1/a_2$ and $\beta=a_3/a_2$.

The effective interaction derived above is strongly direction dependent and is crucial to describe the domain wall orientations. Similar anisotropic interactions have been considered in context of martensitic transformations.[9,10]

As we wish to study heterogeneous nucleation, a dynamical formalism is needed to describe the nonequilibrium effects associated with domain switching. Here the TDGL model for the polarization fields is used. We introduce rescaled time variables $t^*=(t|\alpha_1|L)$ $(\alpha_1<0)$ (L is the kinetic coefficient) and space variable $\vec{r}^*=\vec{r}/\phi$ $(\phi=\sqrt{g_1/a|\alpha_1|})$, where a is a dimensionless constant. The polarization field is transformed as $P_x=P_Ru$ and $P_y=P_Rv$, where $P_R=\sqrt{|\alpha_1|/\alpha_{11}}$ is the remnant polarization of the homogeneous state without elastic effects. With this set of normalized parameters, the dimensionless TDGL equations are given as

$$u,_{t^*}=u-u^3-duv^2+au,_{x^*x^*}+bu,_{y^*y^*}+cv,_{x^*y^*}+\epsilon_x+e_x-\gamma u\int d\vec{k}^*H(\vec{k}^*)\Gamma(\vec{k}^*)\exp(-i\vec{k}^*\cdot\vec{r}^*),$$

$$v,_{t^*}=v-v^3-dvu^2+av,_{y^*y^*}+bv,_{x^*x^*}+cu,_{x^*y^*}+\epsilon_y+e_y+\gamma v\int d\vec{k}^*H(\vec{k}^*)\Gamma(\vec{k}^*)\exp(-i\vec{k}^*\cdot\vec{r}^*). \tag{13}$$

Here, $\vec{e}=\vec{E}_{ext}/(P_R|\alpha_1|)$ is the rescaled external electric field and $\vec{\epsilon}$ is the rescaled electric field due to the dipoles, with $q^*_0(\vec{r}^*)=[q_0(\vec{r})/P_R\phi^2|\alpha_1|]$. The constants defined are $b=(g_2/|\alpha_1|\phi^2)$, $c=(g_3/|\alpha_1|\phi^2)$, $d=(\alpha_{12}/\alpha_{11})$, and $\gamma=(q_2^2/\alpha_{11}\phi^2a_2)$. The quantity $\Gamma(\vec{k}^*)$ is the Fourier transform of (u^2-v^2).

We now describe the details of our simulations on the switching behavior. Equation (13) is discretized using the Euler scheme on a 128×128 grid. Periodic boundary conditions are applied in both x^* and y^* directions, corresponding to a clamped infinite system. The space discretization step $\Delta x^*=\Delta y^*=1$ and the time interval $\Delta t^*=0.02$. The parameter values chosen for the simulation are $d=0.5$ and $\gamma=0.05$. The gradient coefficients are chosen as $a=b=c=2$. Similarly, we choose the elastic parameters as $\alpha=\beta=1$. For the defect field $\vec{\epsilon}$, we take q^*_0 to be uniformly distributed in the interval $[0.01,0.03]$. The charge separation $\vec{\delta}^*$ can take the value $(\pm c,0)$ or $(0,\pm c)$, where c is a random number uniformly distributed in the interval $[0.08,0.1]$. The defect field is initialized by selecting random points on the discrete grid. We choose the number of defects to be $n_d=81$ ($\sim0.5\%$ of the total points on the discrete grid). Then, the electric field due to these defects is calculated at each grid point. We start the simulations by taking a trial single-domain configuration $u(\vec{r}^*,t^*=0)=4$, $v(\vec{r}^*,t^*=0)=0$, and $e_x(t=0)=25$. Under the external electric field, the trial configuration rapidly evolves into a single-domain state with the polarization in the positive x^* direction (except in the vicinity of the defects, where the polarization field is distorted, according to the defect field). After every interval of $t^*_w=50$ (2500 iterations), the electric field is changed with time as $e_x(t^*)=25-50(t^*/t^*_{max})$, where $t^*_{max}=10\,000$ is the total number of time steps. Figure 1 displays sequence of domain snapshots for different values of t^* and e_x. The direction of the arrow shows the local polarization direction and the length of the arrows is proportional to the magnitude of $\vec{P}$. In Fig. 1(a), we can see a single domain poled along the $+x^*$ direction, corresponding to $t^*=4499$ and e_x

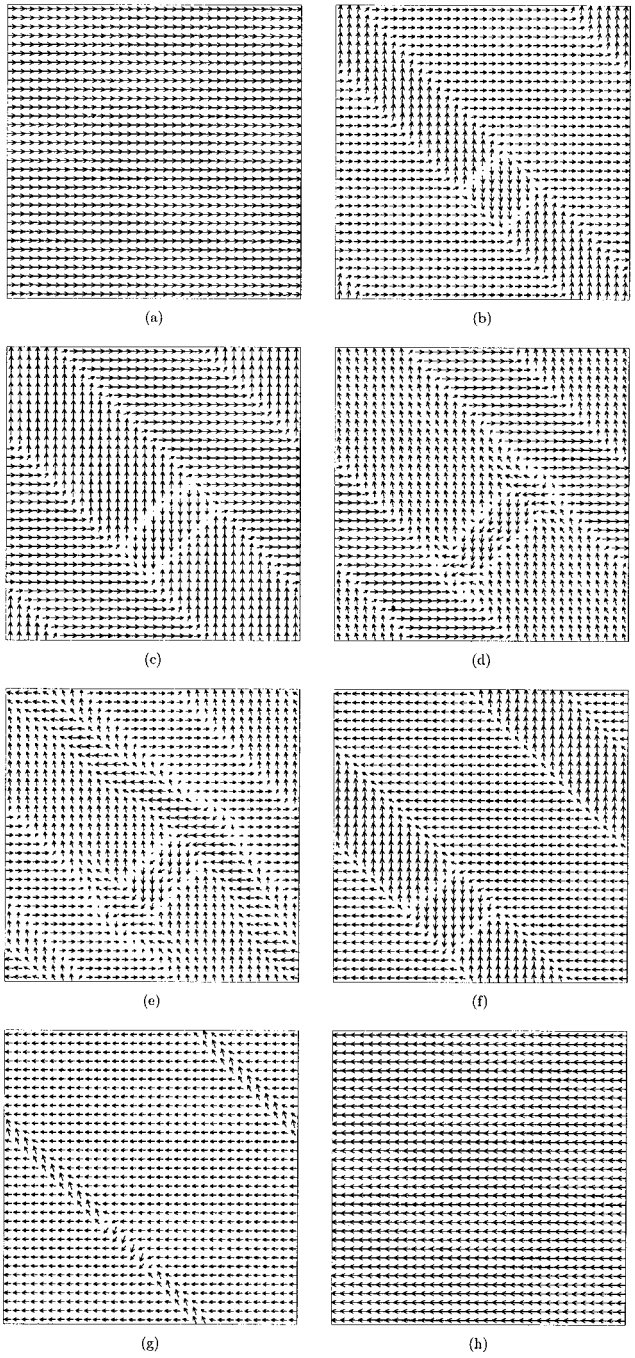

FIG. 1. Pattern evolution for the simulated quasistatic switching. The snapshots correspond to (a) $t^*=4499$, $e_x=2.75$; (b) $t^*=4749$, $e_x=1.5$; (c) $t^*=5049$, $e_x=0$; (d) $t^*=5110$, $e_x=-0.5$; (e) $t^*=5115$, $e_x=-0.5$; (f) $t^*=5249$, $e_x=-1$; (g) $t^*=8499$, $e_x=-17.25$; (h) $t^*=9249$, $e_x=-21$.

$=2.75$. However, at defect sites, polarization inhomogeneities are observed. As we quasistatically decrease the field further, we find that the polarization decreases almost instantaneously in response to change in e_x. However, as the field value reaches $e_x=2$, some of the polarization inhomogeneities nucleate orthogonally polarized domains. In Fig. 1(b) ($t^*=4749$, $e_x=1.5$), we can see a well-developed domain pattern with 90° as well as 180° twin boundaries. Notice that there are head to head as well as head to tail configurations. This is in agreement with recent experiments where charged domain walls have been observed in bulk multidomain single crystals.[11] It is believed that charged domain walls may be stabilized due to charged defects. On decreasing the field further, the orthogonally polarized domains grow by sideways motion. The 180° domain walls also move in order to get rid of head-head and tail-tail domain walls. This growth can be clearly seen by comparing Fig. 1(b) with Fig. 1(c) (corresponding to $t^*=5049$ and $e_x=0$). Figures 1(d) ($t^*=5110$) and 1(e) ($t^*=5115$) show the nucleation and growth of domains with reversed polarization when the field value becomes $e_x=-0.5$. It is clear that these domains nucleate at the 90° twin boundaries. The nucleation of reverse polarization domains from 90° twin boundaries has indeed been observed in recent experiments on lead zirconate titnate thin films.[12] The nucleated reverse domains grow anisotropically along the twin boundary, as reported in the experiments of Ganpule *et al.*[12] As we can see, contrary to the classical picture of 180° polarization flipping, the growth of reversed domains occurs by 90° reorientations in our simulations. Figure 1(f) shows the domain pattern at $t^*=5249$ and $e_x=-1$. Thus, even beyond the coercive field ($e_c \sim -0.5$), complete reversal is not achieved as the defects tend to pin the domain pattern. In Fig. 1(g) we can see that at $t^*=8499$ and $e_x=-17.25$. The reversed polarization domains grow sideways at the expense of orthogonally polarized domains. Finally, when the external field is high enough, we get a single-domain state of the reversed phase as shown in Fig. 1(h) ($t^*=9249$, $e_x=-21$). We continue decreasing the field until $t^*=t^*_{max}$ and $e_x=-25$. The reverse cycle is studied by increasing the field in the same way until $e_x=25$, starting from the final single-domain configuration at $e_x=-25$.

The hysteresis loop, obtained by computing the average x^* component of the rescaled polarization $\langle u \rangle$, is plotted in Fig. 2(a). Also plotted in Fig. 2(a) is the hysteresis loop corresponding to the case without defects. We observe that due to the nucleation of 90° domains, the coercive field for the loop with defects is less than half of the coercive field for the defect-free case. It is also interesting to note that within the range shown in Fig. 2(a), the curves for the defect-free case and the case with defects do not coincide. We have to go to much higher field values for the two curves to match. This is due to the fact that defects pin the domain walls. Another interesting consequence of the dipolar defects is the dependence of the hysteresis loop on the waiting time t^*_w. In Fig. 2(b), we plot the hysteresis loops obtained from identical simulations but with different values of waiting times. We can see that the coercive field seems to increase as the waiting time is decreased. This behavior has also been observed in experiments on ceramics and single crystals.[13,14] The waiting time dependence can be understood on the basis of the defect nucleation mechanism. If the waiting times are short, the nucleated domains have no time to grow, thereby delaying the switching process.

To summarize, we have studied the influence of dipolar

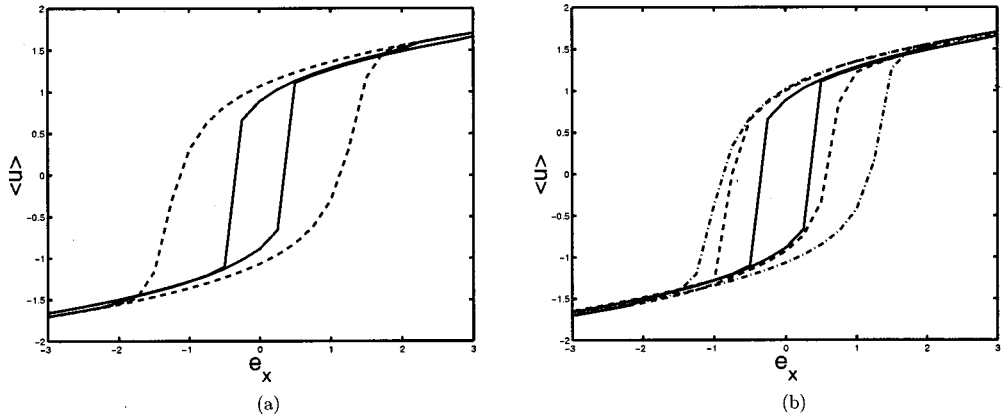

FIG. 2. Plots of $\langle u \rangle$ vs e_x showing the hysteresis loops: (a) the simulated loops for the case with defects (solid line) and the defect-free case (dashed line); (b) the waiting time dependence of the loops for the case with defects for $t_w^*=50$ (solid line), $t_w^*=5$ (dashed line), and $t_w^*=1$ (dot-dashed line).

defects on switching in ferroelectrics, based on the TDGL approach. We find that defects have a remarkable effect on the hysteresis; in particular, the coercive field is reduced due to nucleation events which assist the polarization reversal. We also find that switching occurs by successive 90° rotations for a clamped system. Recent ultrasonic measurements[15] on PZN-PT single crystals have demonstrated that such a mechanism may indeed be occurring in some ferroelectrics. We also observe the dependence of the coercive field on waiting time, in accordance with several reported experiments.

This research was supported by the Office of Naval Research.

[1] M. E. Lines and A. M. Glass, *Principles and Applications of Ferroelectrics and Related Materials* (Clarendon, Oxford, 1979).
[2] Stephen Ducharme, V. M. Fridkin, A. V. Bune, S. P. Palto, L. M. Blinov, N. N. Petukhova, and S. G. Yudin, Phys. Rev. Lett. **84**, 175 (2000).
[3] S. C. Hwang and G. Arlt, J. Appl. Phys. **87**, 869 (2000).
[4] S. Nambu and D. A. Sagala, Phys. Rev. B **50**, 5838 (1994).
[5] Hong-Liang Hu and Long-Qing Chen, Mater. Sci. Eng., A **238**, 182 (1997).
[6] Wenwu Cao, S. Tavener, and S. Xie, J. Appl. Phys. **86**, 5739 (1999).
[7] Wenwu Cao and L. E. Cross, Phys. Rev. B **44**, 5 (1991).
[8] E. A. H. Love, *A Treatise on the Mathematical Theory of Elasticity* (Dover, New York, 1944), p. 49.
[9] S. Kartha, J. A. Krumhansl, J. P. Sethna, and L.K. Wickham, Phys. Rev. B **52**, 803 (1995).
[10] S. R. Shenoy, T. Lookman, A. Saxena, and A. R. Bishop, Phys. Rev. B **60**, R12 537 (1999).
[11] Jianhua Yin and Wenwu Cao, J. Appl. Phys. **87**, 7438 (2000).
[12] C. S. Ganpule, V. Nagarajan, H. Li, A. S. Ogale, D. E. Steinhauer, S. Aggarwal, E. Williams, R. Ramesh, and P. De Wolf, Appl. Phys. Lett. **77**, 292 (2000).
[13] Yun-Han Chen and Dwight Viehland, Appl. Phys. Lett. **77**, 133 (2000).
[14] Jianhua Yin and Wenwu Cao (unpublished).
[15] Wenwu Cao and Jianhua Yin (unpublished).